Mol Neurobiol (2018) 55:980–988
DOI 10.1007/s12035-017-0383-z

Maternal Hypermethioninemia Affects Neurons Number, Neurotrophins Levels, Energy Metabolism, and Na^+,K^+-ATPase Expression/Content in Brain of Rat Offspring

Bruna M. Schweinberger[1] · André F. Rodrigues[1] · Elias Turcatel[1] · Paula Pierozan[1] · Leticia F. Pettenuzzo[1] · Mateus Grings[1] · Giselli Scaini[2] · Mariana M. Parisi[1] · Guilhian Leipnitz[1] · Emilio L. Streck[2] · Florencia M. Barbé-Tuana[1] · Angela T. S. Wyse[1]

Received: 12 July 2016 / Accepted: 4 January 2017 / Published online: 13 January 2017

Abstract In the current study, we verified the effects of maternal hypermethioninemia on the number of neurons, apoptosis, nerve growth factor, and brain-derived neurotrophic factor levels, energy metabolism parameters (succinate dehydrogenase, complex II, and cytochrome c oxidase), expression and immunocontent of Na^+,K^+-ATPase, edema formation, inflammatory markers (tumor necrosis factor-alpha and interleukin-6), and mitochondrial hydrogen peroxide levels in the encephalon from the offspring. Pregnant Wistar rats were divided into two groups: the first one received saline (control) and the second group received 2.68 μmol methionine/g body weight by subcutaneous injections twice a day during gestation (approximately 21 days). After parturition, pups were killed at the 21st day of life for removal of encephalon. Neuronal staining (anti-NeuN) revealed a reduction in number of neurons, which was associated to decreased nerve growth factor and brain-derived neurotrophic factor levels. Maternal hypermethioninemia also reduced succinate dehydrogenase and complex II activities and increased expression and immunocontent of Na^+,K^+-ATPase alpha subunits. These results indicate that maternal hypermethioninemia may be a predisposing factor for damage to the brain during the intrauterine life.

Keywords Brain · Maternal hypermethioninemia · Energy metabolism · Na^+,K^+-ATPase · Neurons number · Neurotrophins

Introduction

Elevation in plasma methionine (Met) levels is defined as hypermethioninemia and may occur in some genetic abnormalities. Deficiency of methionine adenosyltransferase I/III is the most usual cause for isolated hypermethioniemia. Other hereditary causes for this condition include classical homocystinuria, deficiencies of citrin, glycine *N*-methyltransferase, *S*-adenosylhomocysteine hydrolase, and fumarylacetoacetate hydrolase. Hypermethioninemia of non-genetic origin occurs during liver disease and excessive consumption of proteins [1].

It is well known that patients with severe hypermethioninemia may present a variable degree of neurological pathology, including mental retardation, cognitive deficit, and cerebral edema [1, 2]. However, little is known about the effect of maternal hypermethioninemia on the neurodevelopment during intrauterine life. In this context, we have recently shown that increased Met levels during rat gestation reduces Na^+,K^+-ATPase activity and induces oxidative stress in the encephalon of the pups [3].

As a consequence of these alterations, neuronal necrosis may occur [4, 5]. Therefore, evaluation of programmed cell death and quantification of neurons are very important to test this hypothesis and determine Met toxicity. In addition to

✉ Angela T. S. Wyse
wyse@ufrgs.br

[1] Postgraduate Program in Biological Sciences—Biochemistry, Department of Biochemistry, Institute of Health Basic Sciences, Federal University of Rio Grande do Sul, Rua Ramiro Barcelos, 2600-Anexo, CEP, Porto Alegre, RS 90035-003, Brazil

[2] Postgraduate program in Health Sciences, Laboratory of Bioenergetics, University of Southern Santa Catarina, Criciúma, SC, Brazil

these parameters, the measurement of neurotrophic factors levels could be helpful to identify another potential mechanism that may contribute to neurological damage during maternal hypermethioninemia since the reduction in these molecules levels may impair growth, survival, and/or differentiation of neurons [6].

Met induces oxidative stress and decreases Na^+,K^+-ATPase activity, an enzyme highly dependent on an adequate supply of ATP [7]. An increased reactive oxygen species production may cause energy metabolism impairment and also contribute to inflammatory responses [8].

This work aimed to evaluate in brain of pups born to hypermethioninemic rats: neurons number; apoptosis-related proteins (Bax, Bcl-2, Bcl-xL, p53); nerve growth factor (NGF) and brain-derived neurotrophic factor (BDNF) content; succinate dehydrogenase (SDH), complex II, and cytochrome c oxidase (COX) activities; Na^+,K^+-ATPase expression/immunocontent; edema; tumor necrosis factor-alpha (TNF-alpha), interleukin-6 (IL-6), and hydrogen peroxide (H_2O_2) levels.

Materials and Methods

Animals and Reagents

Wistar rats were acquired from the Central Animal House of the Departamento de Bioquímica, Instituto de Ciências Básicas da Saúde, Universidade Federal do Rio Grande do Sul, Porto Alegre, RS, Brazil. Animals were maintained on a 12:12 h light/dark cycle in constant temperature (22 ± 1 °C) and had free access to a 20% (*w*/*w*) protein commercial chow and water. Experiments followed the NIH "Guide for the Care and Use of Laboratory Animals" (NIH publication No. 80–23, revised 1996) and the official governmental guidelines in compliance with the Federação das Sociedades Brasileiras de Biologia Experimental. This research project was approved by the Ethics Committee in Research of Universidade Federal do Rio Grande do Sul (protocol number 25913).

Chemicals were acquired from Sigma Chemical Co., St. Louis, MO, USA.

Chronic Methionine Treatment

After mating the female rats with males, pregnancy was presumed by the presence of sperm in the vaginal smear. During the gestational period (around 21 days), the pregnant rats (70 to 90 days of age) received two daily subcutaneous injections of 2.68 μmol Met/g body weight. Control rats received saline. After birth, pups were killed at the 21st day of life [3]. After decapitation, encephalon was immediately removed and kept chilled until homogenization.

Number of Neurons

Tissues were dissociated with PBS/Collagenase, washed with PBS, and then suspended in PBS/collagenase. After, the cell was permeabilized with 0.2% PBS Triton X-100 at room temperature for 10 min and blocked with BSA 5% for 15 min. Cells were incubated in blocking solution containing the monoclonal antibodies anti-NeuN (clone A60) diluted 1:100 during 2 h. The cells were washed with PBS and incubated for 1 h in blocking solution containing Alexa Fluor 488-anti-rabbit IgG diluted 1:200. The levels of positive NeuN cells were determined by flow cytometry (FACSCalibur, Becton Dickinson, Franklin Lakes, NJ, USA). Alexa Fluor 488 was excited at 488 nm using an air-cooled argon laser. Samples with the secondary antibody (negative controls) were included for setting up the machine voltages. Controls stained with a single dye were used to set compensation. The emission of fluorochromes was recorded through specific band-pass fluorescence filter green (FL-1; 530 nm/30). Fluorescence emissions were collected using logarithmic amplification. Data from 10,000 events were acquired, and the mean relative fluorescence intensity was determined after exclusion of debris events from the data set. Flow cytometric acquisitions and analyzes were performed through Flow Jo software 7.6.3 (Treestar, Ashland, OR). The proportion of cells stained with NeuN was expressed as percentage of control.

Apoptosis

Samples were homogenized in Laemmli-sample buffer (62.5 mM Tris–HCl, pH 6.8, 1% (*w*/*v*) SDS, 10% (*v*/*v*) glycerol). The same quantities of protein (30 μg/well) were fractionated by 10–15% SDS-polyacrylamide gel and electroblotted onto nitrocellulose membranes. Electro-blotting efficiency and protein loading were verified through Ponceau S staining. Membranes were blocked in Tween-Tris buffered saline (100 mM Tris-HCl, pH 7.5, containing 0.9% NaCl and 0.1% Tween-20) containing 5% albumin. Then, membranes were incubated overnight at 4 °C with rabbit polyclonal antibody against Bcl-2 (Cell Signaling – 2876), Bax (Cell Signaling – 2772), Bcl-xL (Cell Signaling – 2762), and p53 (Cell Signaling – 9282). The primary antibody was removed, and membranes were washed four times during 15 min. Then, an anti-rabbit IgG peroxidase-linked secondary antibody was incubated with the membranes for 1 h (diluted 1:10,000), and membranes were washed once more. Lastly, the immunoreactivity was verified through an enhanced chemiluminescence ECL Plus kit. After exposure, membranes were stripped and incubated with a mouse monoclonal antibody to β-Actin (Sigma – A2228) in the presence of 5% milk. An anti-mouse IgG peroxidase-linked secondary antibody was incubated with the membranes during 1 h (diluted 1:10,000), and the membranes were washed once more. Immunoreactivity

was verified through an enhanced chemiluminescence ECL Plus kit. Densitometry was executed through Image J v.1.34 software, and SeeBlue ® Plus2 Prestained Standard (Invitrogen) was utilized as a molecular weight marker to provide certainty that the right bands were analyzed for proteins.

Nerve Growth Factor Levels

Brain tissue was homogenized in PBS (Laborclin, Paraná, Brazil) with a protease inhibitor cocktail (Sigma-Aldrich, St. Louis, MO, USA). NGF levels were determined using a sandwich-ELISA assay with monoclonal antibodies for NGF (Millipore, USA and Canada). Microtitre plates (96-well flat-bottom) were coated during 24 h with the samples (diluted 1:2) and a standard curve (15.6 to 1000 pg/ml of NGF). The plates were washed four times with the sample diluent. Next, a monoclonal anti-NGF mouse antibody (diluted 1:1000) was added to each well and incubated during 2 h at room temperature. Then, a peroxidase-conjugated anti-rabbit antibody (diluted 1:1000) was added to each well and incubated for 2 h at room temperature. After addition of streptavidin enzyme, substrate, and stop solution, NGF levels were determined by measuring the absorbance at 450 nm. The standard curve indicated a relationship between optical density and NGF levels.

Energy Metabolism

Encephalon was homogenized (1:20, *w*/*v*) in SETH (250 mM sucrose, 2 mM EDTA, 10 mM Trizma base, 50 UI mL^{-1} heparin) buffer, pH 7.4. The homogenates were centrifuged at 800×*g* for 10 min, and the supernatants were kept frozen until determinations.

Succinate Dehydrogenase Activity

SDH activity was measured as described by Fischer and collaborators [9]. Samples were frozen and thawed three times to break mitochondrial membranes. The enzymatic activity was determined following the decrease in absorbance due to the reduction of 2,6-dichloroindophenol at 600 nm with 700 nm as reference wavelength (ε = 19.1 mM^{-1} cm^{-1}) in the presence of phenazine methasulfate. The reaction mixture containing 40 mM potassium phosphate, pH 7.4, 16 mM succinate and 8 μM 2,6-dichloroindophenol was preincubated with 40–80 μg homogenate protein for 20 min at 30 °C. Then, 4 mM sodium azide, 7 μM rotenone, and 40 μM 2,6-dichloroindophenol were added. After adding 1 mM phenazine methasulfate, the reaction initiated and was monitored for 5 min.

Complex II (Succinate: 2,6-Dichloroindophenol Oxireductase) Activity

Homogenates are following the decrement in absorbance due to the reduction of 2,6-dichloroindophenol at 600 nm with 700 nm as reference wavelength (ε = 19.1 mM^{-1} cm^{-1}), in accordance to Fischer et al. [9]. The reaction mixture containing 40 mM potassium phosphate, pH 7.4, 16 mM succinate, and 8 μM 2,6-dichloroindophenol was pre-incubated with 40–80 μg homogenate protein for 20 min at 30 °C. After, 4 mM sodium azide and 7 μM rotenone were added. After adding 40 μM 2,6-dichloroindophenol, the reaction initiated and was monitored for 5 min.

Cytochrome c Oxidase

COX activity was measured according to Rustin and colleagues [10]. The activity of this enzyme was determined at 25 °C for 10 min by following the decrease in absorbance due to oxidation of previously reduced cytochrome *c* at 550 nm with 580 nm as reference wavelength (ε = 19.1 $mM^{-1} \times cm^{-1}$). The reaction buffer consisted of 10 mM potassium phosphate, pH 7.0, 0.6 mM *n*-dodecyl-β-D-maltoside, 2–4 μg homogenate protein. Reaction initiated after addition of 0.7 μg reduced cytochrome *c*.

Gene Expression Analyzes

The analysis of ATPase isoforms alpha1 (Atp1a1), alpha2 (Atp1a2), and alpha3 (Atp1a3) expression were performed by quantitative real-time PCR using SYBR Green (Molecular Probes) as the fluorescent detector and glyceraldehyde-3-phosphate dehydrogenase (GAPDH) as the housekeeping gene. Gene sequences available from free databanks (www.ncbi.nlm.nih.gov and www.ensembl.org) were used for primers design with a free software (www.idtdna.com) (Table 1).

Animals were euthanized, and cerebral tissue was immediately frozen in liquid nitrogen and subsequently stored at −80 °C. mRNA was extracted using TRIZOL reagent. RNA was measured in a biophotometer (Eppendorf) at 260/280 nm, and the integrity was confirmed by electrophoresis in a 1% formamide-agarose gel. Complementary DNA (cDNA) was synthesized with M-MLV reverse transcriptase enzyme (Sigma) from 2 μg of total RNA. Three μl of diluted cDNA (1:10) were used as template for PCR reactions with Platinum® Taq Polymerase (Invitrogen) in a final volume of 20 μl. The thermal cycling profile was an initial denaturation at 94 °C for 10 min followed by 40 cycles of 15 s at 94 °C, 15 s at 60 °C, 15 s at 72 °C for data acquisition. The specificity of amplification and absence of primer-dimer was confirmed using melting curve analysis at the end of each run. We also confirmed the amplification of a single amplicon of the

Table 1 Primers sequence of Atp1a1, Atp1a2, ATP1a3, and GAPDH

Name	RefSeq (mRNA)	Ensembl ID	Primer sequence	Amplicon size	
Atp1a1	NM_ 012504	ENSRNOG00000030019	Forward	CTGCTTTCCTGTCC TACTGC	125 bp
			Reverse	CTTCCGCACCTCGT CATAC	
Atp1a 2	NM_ 012505	ENSRNOG00000007290	Forward	GAGGACGAACCATC CAATGAC	133 bp
			Reverse	CTAGGCACCATGTT CTTGAAGG	
Atp1a 3	NM_ 012506	ENSRNOG00000020263	Forward	TTAAGTGCATCGAG CTGTCC	142 bp
			Reverse	AGGTATCGGTTGTC ATTGGG	
GAPDH	NM_ 017008	ENSRNOG00000018630	Forward	GGTGATGCTGGTGC TGAGTA	272 bp
			Reverse	ACTGTGGTCATGAG CCCTTC	

expected size by agarose gel electrophoresis. All reactions were carried out in a StepOnePlus® real-time PCR system (Applied Biosystems). For ΔΔCT analysis [11], samples were normalized by the constitutive gene (GAPDH) and calibrated by the average of the ΔCT of the group itself. Similar specific gene reaction efficiencies were confirmed before the ΔΔCT analysis was done.

Immunocontent of Na^+,K^+-ATPase and Brain-Derived Neurotrophic Factor

Tissues from the brain were homogenized in lysis solution (Tris-HCl 20 Mm). For electrophoresis, samples were dissolved in Laemmli buffer 2× (4% SDS, 20% glycerol, 120 mM Tris-HCl, pH 6.8) and boiled during 3 min. Total protein homogenate was analyzed in 10% SDS-PAGE (30 μg total protein/lane) and transferred (Trans-blot SD semi-dry transfer cell; Bio-Rad, Hercules, CA) to nitrocellulose membranes for 1 h at 15 V in transfer buffer (48 mM Trizma, 39 mM glycine, 20% methanol, and 0.25% SDS). Blots were incubated in blocking solution (TBS plus 5% bovine serum albumin) during 2 h. Subsequently, blots were washed twice with TBS 0.05% Tween-20 (T-TBS) for 5 min and incubated overnight at 4 °C in blocking solution containing one of the following antibodies: monoclonal anti-Na^+,K^+-ATPase (alpha1 subunit) clone M8-P1-A3 obtained from Sigma, Na^+,K^+-ATPase alpha2-isoform from Millipore (Billerica, MA, USA), monoclonal anti-Na^+-K^+-ATPase (alpha3 subunit) clone XVIF9-G10 obtained from Sigma diluted 1:5000, and polyclonal anti-BDNF obtained from Abcam (Cambridge, MA, USA). Membranes were washed twice during 5 min with T-TBS and incubated for 3 h in a solution containing polyclonal peroxidase-conjugated rabbit anti-mouse IgG (1:5000) or polyclonal peroxidase-conjugated anti-rabbit IgG (1:5000). Membranes were washed twice with T-TBS during 5 min and twice with TBS for 5 min. Membranes were developed with the chemiluminescence ECL kit (Amersham, Oakville, Ontario).

Cerebral Edema

After decapitation, brains were removed and immediately weighted. Each sample was dehydrated during 24 h at 110 °C. Then, the weight was measured again and its water content was calculated through the following formula: ((wet weight) − (dry weight)/wet weight) × 100 [12].

Inflammatory Parameters

TNF-alpha and IL-6 levels were quantified by a high-sensitivity ELISA with commercial kits (Invitrogen®). The amounts of these cytokines were measured through an optical densitometry at 450 nm in SpectraMax M5 Microplate Reader (Molecular Devices, Sunnyvale, CA, USA).

Mitochondrial Hydrogen Peroxide Release

Forebrain mitochondria were isolated from the pups as described by Rosenthal and collaborators [13] with slight modifications. After decapitation, brains were rapidly removed and put into ice-cold isolation buffer containing 225 mM mannitol, 75 mM sucrose, 1 mM EGTA, 0.1% bovine serum albumin (free of fatty acids), and 10 mM HEPES, pH 7.2. The forebrain was cut into small pieces, extensively washed, and homogenized 1:10 in a Dounce homogenizer using both a loose-fitting and a tight-fitting pestle. The homogenate was centrifuged during 3 min at 2000*g*. The supernatant was centrifuged during 8 min at 12,000 *g*. The pellet was suspended in isolation buffer

containing 10 μL of 10% digitonin and centrifuged during 8 min at 12,000*g*. The final pellet was washed and suspended in isolation buffer devoid of EGTA. This preparation results in a mixture of synaptosomal and non-synaptosomal mitochondria similar to the brain composition. The mitochondrial preparations (0.5 mg protein mL^{-1}) supported by 2.5 mM glutamate plus 2.5 mM malate were incubated in standard reaction medium in the presence of 10 μM Amplex red and 1 U mL^{-1} horseradish peroxidase. The fluorescence was verified over time on a Hitachi F-4500 spectrofluorometer operated at excitation and emission wavelengths of 563 and 587 nm, respectively, and slit width of 5 nm. Antimycin A (0.1 μg mL^{-1}) was added at the end of the measurement.

Protein Determination

Protein concentration was measured by the method of Lowry and colleagues [14] using bovine serum albumin as standard.

Statistical Determination

Data were analyzed by Student's *t* test. Analyses were performed using the Statistical Package for the Social Sciences (SPSS) software in a PC-compatible computer. Differences were considered statistically significant if $p < 0.05$.

Results

Effect of Gestational Hypermethioninemia on Number of Neurons of the Offspring

As can be seen in Fig. 1, the average labeled neurons was lower in the group of pups whose mothers were treated with Met during gestational period ($T = 4.74$; $p < 0.01$).

Effect of Gestational Hypermethioninemia on Apoptosis in Encephalon of the Offspring

High Met levels during pregnancy had no effect on Bax ($T = 0.49$; $p > 0.05$), Bcl-2 ($T = 2.08$; $p > 0.05$), Bcl-xL ($T = 1.10$; $p > 0.05$), and p53 content ($T = 0.43$; $p > 0.05$) from the encephalon of the offspring (Fig. 2).

Effect of Gestational Hypermethioninemia on Nerve Growth Factor and Brain-Derived Neurotrophic Factor Levels in Encephalon of the Offspring

NGF concentration was determined in the brain, and as can be observed in Fig. 3a, there was a significant reduction in this parameter in pups born to hypermethioninemic mothers ($T = 3.07$; $p < 0.05$). BDNF immunocontent was also decreased ($T = 3.05$; $p < 0.05$) (Fig. 3b).

Effect of Gestational Hypermethioninemia on Energy Metabolism in Encephalon of the Offspring

Figure 4a, b respectively shows that gestational hypermethioninemia significantly decreased SDH ($T = 4.27$; $p < 0.01$) and complex II ($T = 4.98$; $p < 0.01$) activities in the encephalon of the offspring. COX activity was not altered (control: 116.87 ± 23.81; Met: 139.51 ± 42.36).

Effect of Gestational Hypermethioninemia on Expression and Immunocontent of Na^+,K^+-ATPase in Encephalon of the Offspring

Expression of Na^+,K^+-ATPase subunits was higher in the encephalon of the pups whose mothers received Met: alpha1 ($T = 2.89$; $p < 0.05$), alpha2 ($T = 3.27$; $p < 0.01$), and alpha3 ($T = 3.30$; $p < 0.01$) (Fig. 5a). Examination of Na^+,K^+-ATPase alpha subunits by immunoblot also revealed that alpha1 ($T = 2.75$; $p < 0.05$), alpha2 ($T = 3.23$; $p < 0.01$), and alpha3

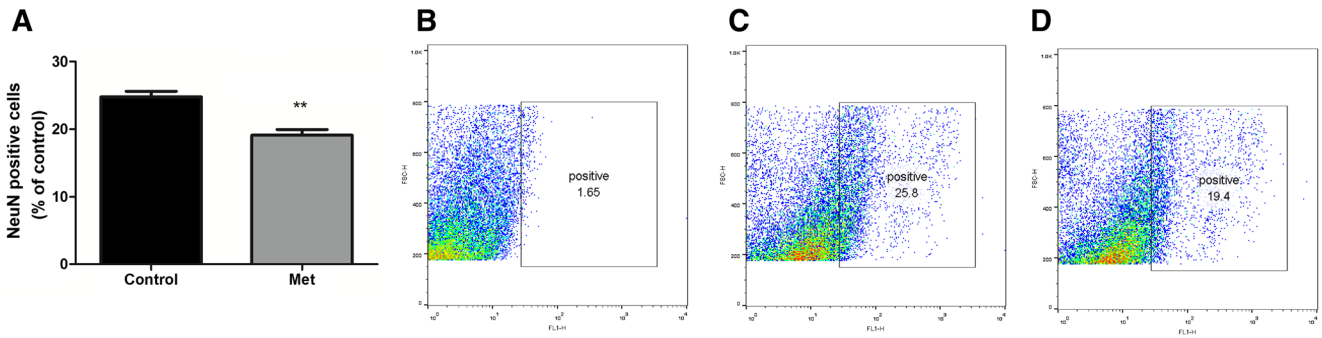

Fig. 1 **a** Graph representing the effect of gestational hypermethioninemia on the number of neurons in the rat pups. Results are expressed as means ± SD for six animals in each group. Different from control, $^{**}p < 0.01$ (Student's *t* test). **b** Representative plot from negative control sample processed without NeuN antibody, just the secondary antibody. **c** Representative plot from control rat. **d** Representative plot from treated rat

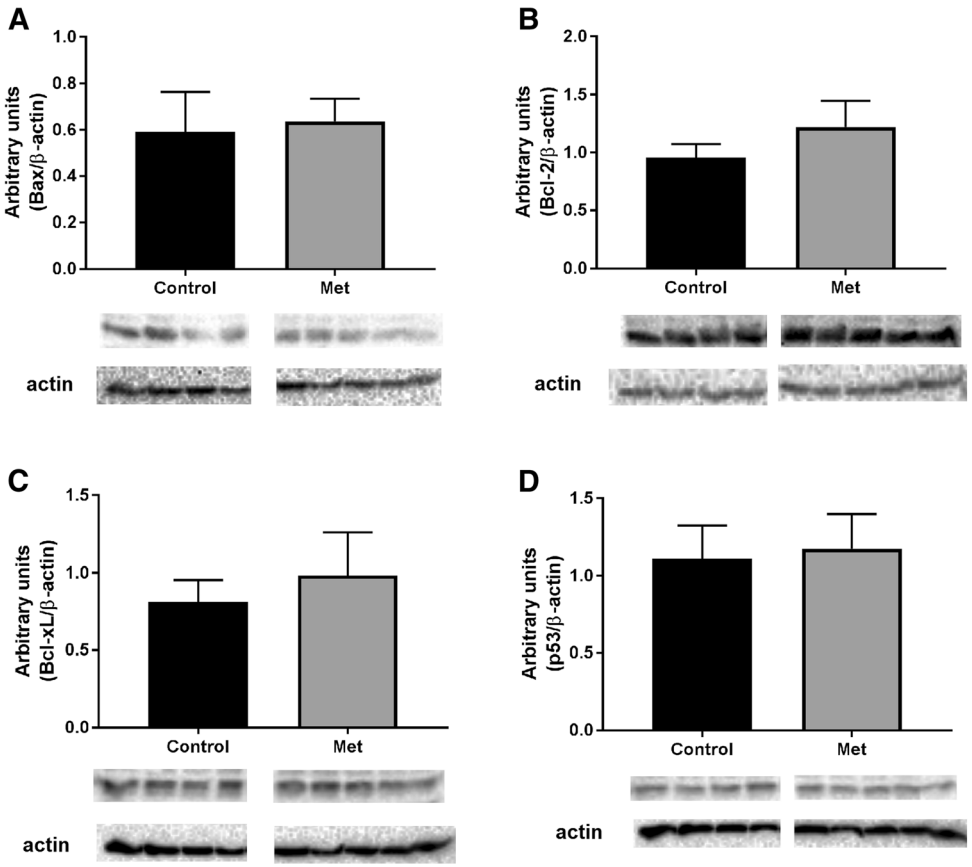

Fig. 2 Effect of gestational hypermethioninemia on Bax (**a**), Bcl-2 (**b**), Bcl-xL (**c**), and p53 (**d**) content in encephalon of the rat pups. Results are expressed as means ± SD for six animals in each group, $p > 0.05$ (Student's t test)

($T = 3.33$; $p < 0.01$) protein content was increased in the encephalon of pups whose mothers were treated with Met, as shown in Fig. 5B.

Effect of Gestational Hypermethioninemia on Cerebral Edema Formation in the Offspring

Determination of tissue water content revealed that maternal hypermethioninemia did not cause cerebral edema in the offspring (control: 77.03 ± 0.65; Met: 76.77 ± 1.41).

Effect of Gestational Hypermethioninemia on Biomarkers of Inflammation in the Encephalon of the Offspring

Gestational hypermethioninemia was not able to significantly alter the levels of TNF-alpha (control: 6.81 ± 1.31; Met: 5.52 ± 0.99) and IL-6 (control:

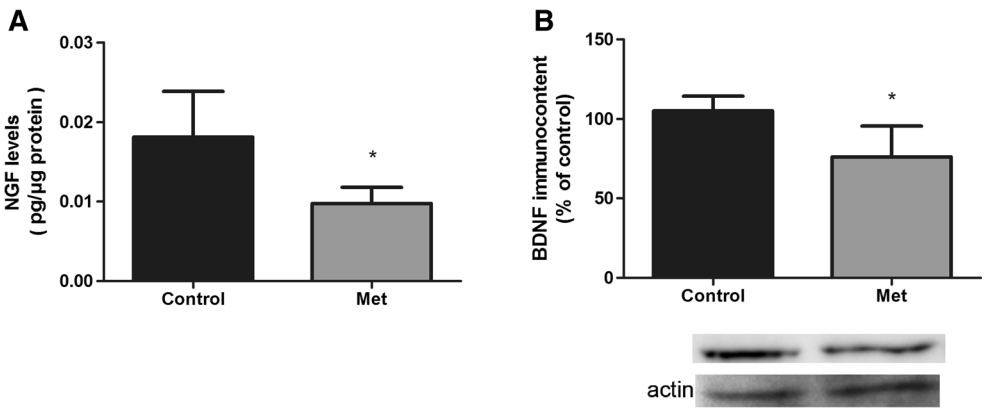

Fig. 3 Effect of gestational hypermethioninemia on NGF (**a**) and BDNF (**b**) levels in encephalon of the rat pups. Results are expressed as means ± SD for six animals in each group. Different from control, $^{*}p < 0.05$ (Student's t test)

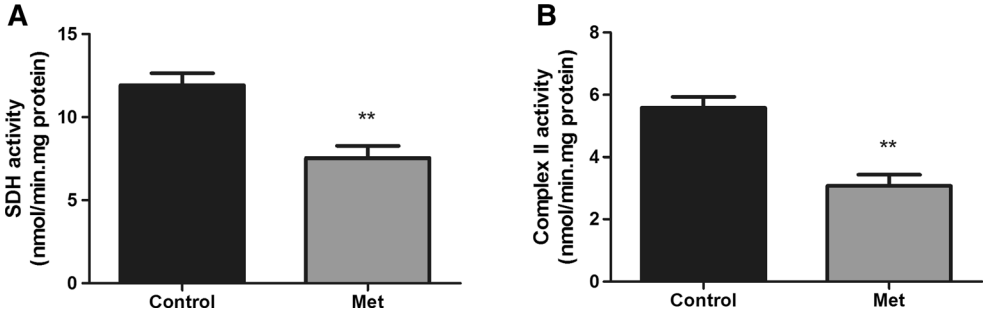

Fig. 4 Effect of gestational hypermethioninemia on SDH (**a**) and complex II (**b**) activities in encephalon of the rat pups. Results are expressed as means ± SD for six animals in each group. Different from control, $^{**}p < 0.01$ (Student's *t* test)

140.67 ± 34.42; Met: 177.33 ± 31.60) in the brain of the offspring.

Effect of Gestational Hypermethioninemia on Mitochondrial Hydrogen Peroxide Levels in the Encephalon of the Offspring

The levels of H_2O_2 were quantified in the encephalon of pups but no difference between the groups was observed (control: 1.82 ± 0.10; Met: 1.85 ± 0.06).

Discussion

Patients with severe hypermethioninemia may present neurological dysfunction manifested by cognitive deficit and mental retardation [1]. However, the effect of the maternal hypermethioninemia on the developing brain during intrauterine life is still poorly studied. Therefore, in the present study, we chemically induced hypermethioninemia in pregnant rats and evaluated the number of neurons, thorough monoclonal antibody anti-NeuN, in the encephalon of the offspring. There was a significant difference between the groups, indicating that maternal hypermethioninemia reduced neurons number. Although we have observed a loss of neuronal cells, neither the pro-apoptotic proteins (Bax and p53) nor the anti-apoptotic proteins (Bcl-2 and Bcl-xL) were altered. This result may suggest that the Met treatment induced apoptosis by a mechanism not dependent on p53 or Bcl-2 family members. Besides, the neuronal loss observed is probably related to the decreased NGF and BDNF content. These neurotrophins have important role in the generation of neurons, as well as in the neuronal survival. These results are very important since decreased number of neurons during brain development can impair synaptic responses and lead to learning problems in the offspring. Besides, NGF and BDNF play a crucial role during the process of memory formation [15, 16].

Next, we evaluated brain energy metabolism. Results showed that SDH and complex II activities were significantly reduced in the encephalon of pups whose mothers were treated with Met, suggesting an impaired respiratory chain function. It was previously reported that maternal hypermethioninemia induces oxidative stress in brain of the offspring [3], and it is well known that the complexes of electron transport chain are susceptible to injury by free radicals [17], which could explain these results. Since complex II/SDH plays a key role in the respiratory chain and the tricarboxylic acid cycle [18, 19] and since the brain is highly dependent on a

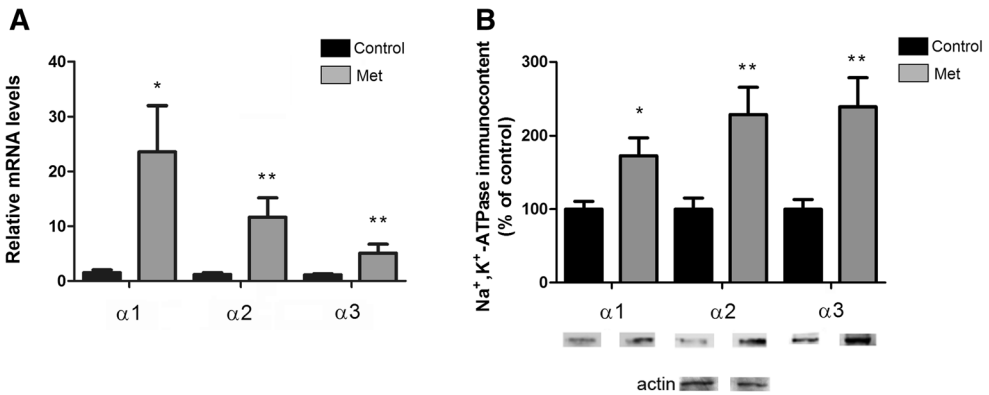

Fig. 5 Effect of gestational hypermethioninemia on the expression (**a**) and immunocontent (**b**) of Na^+,K^+-ATPase alpha1, alpha2, and alpha3 subunits in encephalon of the rat pups. Results are expressed as means ± SD for six animals in each group. Different from control, $^{*}p < 0.05$; $^{**}p < 0.01$ (Student's *t* test)

continuous supply of energy, this condition could cause neurological damage [20]. Studies have shown that reduced energy demand is associated with various neurodegenerative disorders, such as Alzheimer's, Parkinson's, and Huntington's diseases, as well as Friedreich's ataxia [21–23].

It is also important to underline that in our previous work, brain Na^+,K^+-ATPase activity was reduced in pups due to maternal hypermethioninemia [3]. Once this enzyme consumes ATP at a high rate, the reduced complex II/SDH activity could reduce energy supply and consequently contribute to the diminish in the activity of Na^+,K^+-ATPase. To better understand the mechanisms involved in the reduced activity of this enzyme during gestational hypermethioninemia, we also evaluated the expression and immunocontent of Na^+,K^+-ATPase. Results showed that the inhibitory effect of Met on Na^+,K^+-ATPase activity observed in our previous study was inversely correlated to the mRNA levels and immunocontent of the catalytic alpha subunits of Na^+,K^+-ATPase. This result suggests that the Met-induced decrease in Na^+,K^+-ATPase activity does not occur by altering gene expression or the total number of enzyme molecules, but is a post-translational inhibition probably due to reduced energy metabolism and/or oxidative damage to SH groups of Na^+,K^+-ATPase. Besides, the up-regulation in transcription/translation with consequent increase in the amount of the enzyme probably indicates the development of an adaptive compensatory mechanism.

Previous studies have demonstrated that reduced Na^+,K^+-ATPase activity in the brain is able to increase the intracellular Na^+ concentration, contributing to the physiopathological mechanisms involved in the formation of cerebral edema [24]. On this basis, we also evaluated the content of water in the brain of the offspring, but no difference was observed when compared to control. Therefore, although patients with severe hypermethioninemia may present cerebral edema [1], this condition during gestation does not seem to affect the offspring. Studies show that the inactivation of Na^+-K^+-ATPase activity does not necessarily cause an increase in cell volume, since inhibition of Na^+ exit may be rapidly compensated by a reduction in apical Na^+ entry and an improve in basolateral Cl^- conductance [25].

Neuroinflammation has been identified as a factor that contributes to development of neurological diseases, such as Alzheimer's disease [26], Parkinson's disease [27], Huntington's disease [28], and multiple sclerosis [29]. Once enhanced reactive oxygen species production may up-regulate pro-inflammatory process [30] and we demonstrated in our previous work that Met treatment during gestation induces oxidative stress in brain of the offspring [3], we evaluated the effect of this treatment on brain inflammation of rats pups. TNF-alpha is a cell signaling protein that induces the migration of leukocytes to the inflamed tissue and promotes apoptosis [31], while IL-6 is considered an activator of acute phase responses as well as a lymphocyte stimulatory factor [32]. In the present work, we did not observe important alterations in these parameters, suggesting that neuroinflammation is not involved in the pathophysiological process of maternal hypermethioninemia. In agreement, previous studies showed that diet rich in Met does not alter TNF-alpha and IL-6 levels in plasma of mice [33].

We have previously demonstrated that maternal hypermethioninemia decreased catalase activity in the encephalon of the offspring [3]. Once this antioxidant enzyme decomposes H_2O_2, we believed that this condition could increase H_2O_2 levels. However, we measured this reactive oxygen species in the present study and no alteration was observed. It is possible that the action of other peroxidases responsible for H_2O_2 detoxification could have been enough to eliminate this molecule.

In conclusion, we demonstrated for the first time that gestational hypermethioninemia decreases the number of neurons associated to decreased NGF and BDNF levels in brain of the offspring. Maternal hypermethioninemia also reduced SDH and complex II activities and increased gene expression and immunocontent of Na^+,K^+-ATPase. Cerebral edema and neuroinflammation were not observed. These results indicate that maternal hypermethioninemia may be a predisposing factor for damage to the brain during the intrauterine life. Neurological injury during this period could prejudice the developing of central nervous system and cause behavior alterations to the offspring.

Acknowledgments This work was supported in part by grants from Conselho Nacional de Desenvolvimento Científico e Tecnológico (CNPq-Brazil) and Fundação de Amparo à Pesquisa do Estado do Rio Grande do Sul (FAPERGS, RS, Brazil).

Compliance with Ethical Standards

Declaration of Interest The authors declare that they have no conflict of interest.

References

1. Mudd SH, Levy HL, Kraus JP (2001) Disorders of transsulfuration. In: Scriver CR, Beaudet AL, Sly WS, Valle D (eds) The metabolic and molecular bases of inherited disease, 8th edn. McGraw-Hill, New York, pp. 2016–2040
2. Mudd SH, Jenden DJ, Capdevila A, Roch M, Levy HL, Wagner C (2000) Isolated hypermethioninemia: measurements of S-adenosylmethionine and choline. Metabolism 49:1542–1547
3. Schweinberger BM, Schwieder L, Scherer E, Sitta A, Vargas CR, Wyse AT (2014) Development of an animal model for gestational hypermethioninemia in rat and its effect on brain Na^+,K^+-ATPase/Mg^{2+}-ATPase activity and oxidative status of the offspring. Metab Brain Dis 29:153–160
4. Nagafuji T, Koide T, Takato M (1992) Neurochemical correlates of selective neuronal loss following cerebral ischemia: role of decreased Na+,K(+)-ATPase activity. Brain Res 571:265–271

5. Chiurchiù V, Orlacchio A, Maccarrone M (2016) Is modulation of oxidative stress an answer? The state of the art of redox therapeutic actions in neurodegenerative diseases. Oxidative Med Cell Longev 2016:7909380
6. Fields J, Dumaop W, Langford TD, Rockenstein E, Masliah E (2014) Role of neurotrophic factor alterations in the neurodegenerative process in HIV associated neurocognitive disorders. J NeuroImmune Pharmacol 9:102–116
7. Erecinska M, Cherian S, Silver IA (2004) Energy metabolism in mammalian brain during development. Prog Neurobiol 73:397–445
8. Filippin LI, Vercelino R, Marroni NP, Xavier RM (2008) Redox signalling and the inflammatory response in rheumatoid arthritis. Clin Exp Immunol 152:415–422
9. Fischer JC, Ruitenbeek W, Berden JA et al (1985) Differential investigation of the capacity of succinate oxidation in human skeletal muscle. Clin Chim Acta 153:23–36
10. Rustin P, Chretien D, Bourgeron T et al (1994) Biochemical and molecular investigations in respiratory chain deficiencies. Clin Chim Acta 228:35–51
11. Livak KJ, Schmittgen TD (2001) Analysis of relative gene expression data using real-time quantitative PCR and the 2(−Delta Delta C(T)). Method 25:402–408
12. Durmaz R, Ertilav K, Akyüz F, Kanbak G, Bildirici K, Tel E (2003) Lazaroid U-74389G attenuates edema in rat brain subjected to post-ischemic reperfusion injury. J Neurol Sci 215:87–93
13. Rosenthal RE, Hamud F, Fiskum G, Varghese PJ, Sharpe S (1987) Cerebral ischemia and reperfusion: prevention of brain mitochondrial injury by lidoflazine. J Cereb Blood Flow Metab 7:752–758
14. Lowry OH, Rosebrough NJ, Farr AL, Randal RJ (1951) Protein measurement with the folin phenol reagent. J Biol Chem 193: 265–275
15. Zhang H, Petit GH, Gaughwin PM et al (2013) NGF rescues hippocampal cholinergic neuronal markers, restores neurogenesis, and improves the spatial working memory in a mouse model of Huntington's disease. J Huntingtons Dis 2:69–82
16. Bramham CR, Messaoudi E (2005) BDNF function in adult synaptic plasticity: the synaptic consolidation hypothesis. Prog Neurobiol 76:99–125
17. Sverdlov AL, Elezaby A, Behring JB et al (2015) High fat, high sucrose diet causes cardiac mitochondrial dysfunction due in part to oxidative post-translational modification of mitochondrial complex II. J Mol Cell Cardiol 78:165–173
18. Ackrell BA (2000) Progress in understanding structure-function relationships in respiratory chain complex II. FEBS Lett 466:1–5
19. Rustin P, Munnich A, Rötig A (2002) Succinate dehydrogenase and human diseases: new insights into a well-known enzyme. Eur J Hum Genet 10:289–291
20. Bolaños JP, Moro MA, Lizasoain I, Almeida A (2009) Mitochondria and reactive oxygen and nitrogen species in neurological disorders and stroke: therapeutic implications. Adv Drug Deliv Rev 61:1299–1315
21. Ferrer I (2009) Altered mitochondria, energy metabolism, voltage-dependent anion channel, and lipid rafts converge to exhaust neurons in Alzheimer's disease. J Bioenerg Biomembr 41:425–431
22. Ebadi M, Govitrapong P, Sharma S et al (2001) Ubiquinone (coenzyme q10) and mitochondria in oxidative stress of parkinson's disease. Biol Signals Recept 10:224–253
23. Schapira AH (1999) Mitochondrial involvement in Parkinson's disease, Huntington's disease, hereditary spastic paraplegia and Friedreich's ataxia. Biochim Biophys Acta 1410:159–170
24. Kempski O (2001) Cerebral edema. Semin Nephrol 21:303–307
25. Granitzer M, Mountian I, De Smet P, Van Driessche W (1994) Effect of ouabain on membrane conductances and volume in A6 cells. Ren Physiol Biochem 17:223–231
26. Heneka MT, Carson MJ, El Khoury J et al (2015) Neuroinflammation in Alzheimer's disease. Lancet Neurol 14: 388–405
27. Stojkovska I, Wagner BM, Morrison BE (2015) Parkinson's disease and enhanced inflammatory response. Exp Biol Med 240:1387–1395
28. Chang KH, Wu YR, Chen YC, Chen CM (2015) Plasma inflammatory biomarkers for Huntington's disease patients and mouse model. Brain Behav Immun 44:121–127
29. Frohman EM, Racke MK, Raine CS (2006) Multiple sclerosis—the plaque and its pathogenesis. N Engl J Med 354:942–955
30. Martinon F (2010) Signaling by ROS drives inflammasome activation. Eur J Immunol 40:616–619
31. Bradley JR (2008) TNF-mediated inflammatory disease. J Pathol 214:149–160
32. Rath T, Billmeier U, Waldner MJ, Atreya R, Neurath MF (2015) From physiology to disease and targeted therapy: interleukin-6 in inflammation and inflammation-associated carcinogenesis. Arch Toxicol 89:541–554
33. Liu WH, Zhao YS, Gao SY et al (2010) Hepatocyte proliferation during liver regeneration is impaired in mice with methionine diet-induced hyperhomocysteinemia. Am J Pathol 177:2357–2265